Optimization of a suspended two photon polymerized microfluidic filtration system

Optimization of a suspended Two Photon Polymerized microfluidic filtration system

F Perrucci [a], V Bertana [a], S L Marasso [a b], G Scordo [a], S Ferrero [a], C F Pirri [a], M Cocuzza [a b], A El-Tamer [c], U Hinze [c], B N Chichkov [c], G Canavese [d], L Scaltrito [a]

a Chilab - Materials and Microsystems Laboratory - DISAT Politecnico di Torino, Via Lungo Piazza d'Armi 6, 10034 Chivasso (Turin), Italy
b CNR-IMEM, Parco Area delle Scienze 37a, 43124 Parma, Italy
c Laser Zentrum Hannover e.V., Hollerithallee 8, 30419 Hannover, Germany
d Department of Applied Science and Technology, Politecnico di Torino, Corso Duca degli Abruzzi 24, 10129 Torino, Italy
Corresponding author e-mail: valentina.bertana@polito.it

Abstract

Two Photon Polymerization (2PP) is a powerful additive manufacturing technology already employed in the field of micro-/nano- engineering. The resolution achieved by 2PP 3D printing systems is in the range of hundreds of nanometers, but the printing volume is limited to few mm^3 and printing times are not negligible. Therefore, it cannot be considered economically efficient with respect to standard clean room technologies or other Stereolitography (SL) techniques. A possible solution to this limitation is the embedding of micro-/nano- features fabricated by 2PP inside a low-resolution object obtained by SL printers. Moreover, 2PP optimized strategies should be adopted to maximize the resolution and maintain a high printing velocity. In this work, a suspended microfilter obtained by a 2PP system has been successfully integrated in a 3D printed microfluidic structure. The microchannel was fabricated by a standard SL printer using a low-cost 3D printing resin, while the suspended microfilter was obtained using a 2PP Micro-3-Dimensional Structuring System (M3D) and a drop of Femtobond D resin. An innovative printing strategy was carried out to maximize the 2PP resolution and optimize the fabrication time. In particular, the X,Y plan was exploited to build the high-resolution mesh, thus obtaining a suspended microfilter that has a final pores size of 4 µm on a considerable area of 0.5 mm^2 in an only 30 minutes process. Finally, the microfluidic filtration system was carried out and its efficiency was evaluated employing size-controlled fluorescent microparticles.

Keywords

3D printing, 2PP, Microfluidics, Filter, Nanostructures

1. Introduction

In the biological and biomedical field, particles sorting is often a key point both for diagnostic and therapeutic purposes. Among the sorting techniques, label-free is the most attractive since it involves very few preparation steps [1]. Label-free separation is mainly based on the physical properties of the different particles or cells and it can be implemented both with active and passive techniques in microfluidic devices [2]. If the sorting efficiency is adequate for the analysis, passive techniques, as porous filters, are preferable because they do not require additional interfaces with external devices which could introduce challenging coupling of different elements [3]. For applications at the micro-scale, microfabrication represents the favorite solution for filters production since it allows to build customized structures which correctly select the particles to be collected [4].

The simplest filtering structure is a single layer membrane, for instance the one described by Yang et al. in 1999 [5]: it was built by silicon micromachining and was studied to collect airborne particles in gaseous flow with a pore range from 6 to 12 µm. Unfortunately, this approach could seem outdated today, since the design of a filter should not only take into account the particles to retain, but also be easily and fully embeddable inside a microfluidic chip with other components [6]. Moreover, the introduction of polymer technology could overcome the disadvantages linked to silicon processing [3]. In this perspective, 3D printing promises to be an effective alternative to micromachining as it allows to print not only a single-layer filter with the desired geometry, but a multi-layer filtrating device embedded in a more complex microfluidic chip. Many researchers have worked in this direction, implementing processes to build micro- and nano- structures with high resolution additive manufacturing techniques. In this regard, two photon polymerization (2PP) represents one of the most suitable processes to build features with a spatial resolution down to 120 nm [7]. Unfortunately,

the high resolution is achieved at the cost of long processing times. This is the reason why 2PP is frequently combined with faster techniques so that most of the device is obtained by a lower resolution and more efficient approach, while the 3D micro-/nano- feature is printed by 2PP [8], trying to shorten process times [9]. An integration of different fabrication technologies means combining, for example, standard microfluidic fabrication techniques with 2PP to achieve a considerable time and cost reduction, thus maintaining the high resolution capability for the critical features [10]. For example, standard Stereolithography (SL) allows for obtaining micro devices with a resolution of tens or hundreds of micrometers and a higher throughput, with respect to 2PP, employing a low-cost resin. Indeed, previous works [11] have demonstrated the applicability of SL systems to fabricate microfluidics and Lab-On-a-Chip with the advantages to easily pass from the design to the device avoiding the implementation of high cost processes or micromachining technology [12,13]. A similar approach for 3D objects manufacturing by integrating SL and 2PP has been developed in a recent work [14], but this technique is still in its infancy since a multi technology printing system does not exist yet.

In this work, a novel printing strategy exploiting the integration of SL and 2PP technologies to obtain a membrane based microfluidic filtration system has been carried out. Differently with respect to previous works, where the filtering structures were developed on the Z axis to obtain a wall-like single-layer filtrating structure [9,15,16], an horizontal membrane-like multi-layered sieve with pores down to 4 µm was fabricated inside a previously 3D printed microchannel. The adopted novel printing strategy allows for maximizing the printing resolution with respect to printing velocity and then for obtaining a filtrating device with pore dimensions of few microns (e.g. the range of blood cells) avoiding the introduction of supporting structures and optimizing the process to reduce building times. A standard SL was employed to print the bulk microchannel, while micro- /nano- metric structures were fabricated exploiting 2PP. The object printability evaluation was carried out and a microfluidic filtration system was properly fabricated. Finally, to prove the filtering capability, real time sorting tests were conducted using fluorescence microparticles.

2. Experimental

2.1 Microfluidic chip design

The microfluidic filtration system geometry consisted of a single-channel chip with one inlet and one outlet, as reported in Figure 1a. One of the peculiarities of this structure is that no top and bottom enclosure are present: this strategy was adopted to allow a better cleaning [17] of both the channel lumen and, in a second time, of the filter. Moreover, with an open channel, the difficulty of 2PP resin vehiculation to the polymerization site is avoided [18]. The channel was designed to be 300 µm wide and 300 µm deep. Inlet and outlet had different dimensions: while the outlet was a 450 µm diameter hole, the inlet was a 650 µm diameter hole with a 200 µm high step-like feature that creates a slot for the filter and was designed to hold and support it both during printing and filtration (Figure 1a). These dimensions and geometries were chosen in accordance with the 2PP printing setup respecting the constraint on the maximum structure height that the apparatus could print (1.1 mm).

The tridimensional layout of the filter was designed in SolidWorks and then converted in a *.STL file for processing.

2.2 Microfilter design

The microfilter consisted in a 50 µm thick circular structure with 800 µm diameter. Its structure was designed to have two main parts, highlighted in Figure 1b: a solid full ring (grey) and a grid structure (blue and cyan, the actual filter). The 100 µm wide external ring was added to mechanically strengthen the structure and overcome the issue of poor adhesion raised by Baldacchini et al. in a similar work [18]. The full integration inside the 650 µm inlet of the SL printed microfluidic channel was reached by designing the filter to be wider than the inlet. Thus, in the 2PP printing step the laser would describe the ring path inside the microfluidic chip walls allowing a polymerization process at the junction point between the two structures (microfluidics and filter). The second part, enclosed by the outer ring, was composed by two grids: a primary one, in which 20 µm wide rods, extending for the whole microfilter height, formed a matrix of 60 µm wide squared holes. A secondary one, composed by smaller rods orientated alternatively along x and y direction between subsequent layers, which formed a 4 µm porosity inside each of the primary grid holes.

The primary grid (cyan color in Figure 1b) provided mechanical resistance to the whole filter and to the secondary grid (blue color in Figure 1b), which represented the real filtering unit. This geometry was generated to combine high filtering surfaces and mechanical stability at the same time.

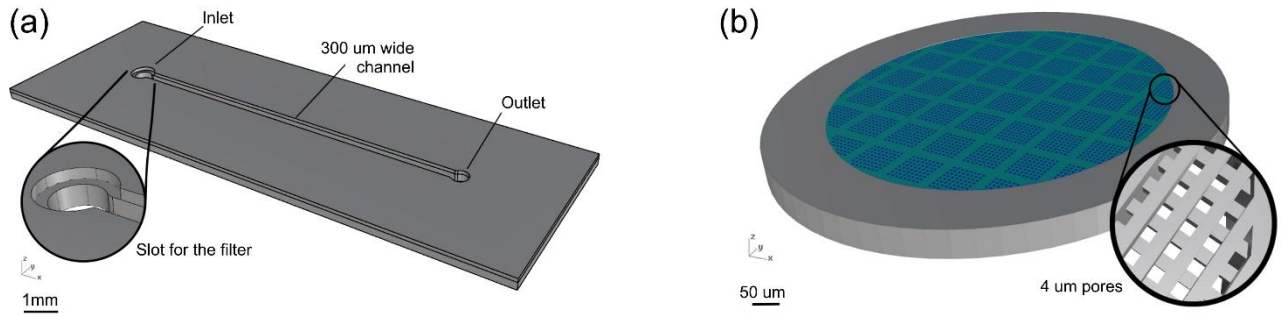

Figure 1 (a) Microfluidic chip geometry (b) Filter geometry: cyan and blue grid represents the filtrating structure while the grey ring the support structure

2.3 Microfluidic chip fabrication

The single channel chip was printed in a SL 3D printer (Microla Optoelectronics s.r.l) equipped with a 405 nm laser source mounted on a galvo scanner. With its minimum feature size of 100 µm on X,Y plane and layer thickness tunable from 20 µm to 200 µm, it can print objects covering a maximum area of 170 x 200 mm^2.

The printing process comprised the following steps: a 175 µm foil of PMMA was positioned on the building platform. This expedient was introduced to perform a better detachment after printing exploiting the lower adhesion of the polymerized resin with PMMA with respect to the building platform material (aluminum). Then, once the resin vat was filled with the commercial resin SpotHT by SpotAmaterials, printing was performed polymerizing the resin layer by layer. In this case, three layers of 100 µm thickness each were printed: the first two had a 450 µm diameter inlet hole while in the last layer a 650 µm concentric hole was polymerized in order to build the step-like feature that would hold the filter. This printer enables the user to set multiple parameters, such as laser power, hatch spacing, hatching pattern and velocity (with different values for internal hatching and borders if desired). The fixed printing parameters (optimized for the SpotHT resin) are reported in Table 1.

Table 1 SL parameters for microfluidic chip printing

Parameter	***Value***
Power	10 mW
Layer Thickness	100 µm
Hatching scan velocity	1000 mm/s
Contour scan velocity	1800 mm/s

After the microfluidic chips were printed, post-curing was performed for 10 minutes under a 24 W UV lamp to ensure all the resin to be fully polymerized.

2.4 Microfilter fabrication

The microfilter was printed with a Micro-3-Dimensional Structuring System (M3D), from Laser Zentrum Hannover (LZH). This system was designed to print micro-/ nano-metric features by 2PP [19] and is equipped with a TOPAG Flint femtosecond laser at 518 nm and a 50x, 0.7 numerical aperture (NA), Zeiss Objective. Before the photo-polymerization process started, the sample was prepared by fixing the microfluidic chip on a microscope slide with tape. A single drop of Femtobond resin was released in the microfluidic inlet with a pipette (Figure 2a) and then a degasification process by low vacuum was performed inside a small chamber to allow air bubble exiting from the resin. Afterward, two PDMS spacers were placed at the inlet sides and used as a support for a coverslip, required to protect the objective from accidental contact with the sample and to flatten the resin surface (Figure 2b). Then, the sample was mounted on the printer holder to find

manually the point where polymerization should start. Finally, the printer started to build the filter by focusing the laser beam inside the resin drop with a scanning speed of 2 mm/s and 45 mW power using a layer thickness of 5 µm.

It should be underlined that the filter printing benefited from the cautious design of the microfluidic channel: the inclusion of a step-like feature inside the inlet helped to avoid the addition of extra supporting structures. The "heaviest" component of the filter represented by the solid full ring was in part polymerized inside and in part supported by the microfluidic walls, while the "lighter" structure represented by the woodpile grid was suspended like a bridge (Figure 2c). Hence, the problem of deformation derived from the attachment to a substrate [20] could be overcome. Moreover, the viscosity of the 2PP resin inside the inlet hole was sufficient to hold the growing filter, until it was self-sustained by the adhesion between the layers and the drum-leather-like tension exerted by the constrained external ring.

At the end of the printing process, the whole device was immersed in 1-propanol and then in ethanol to remove the uncured resin. After that, the solvent was removed from the filter pores by critical point drying: this procedure [21] was used instead of natural drying to avoid stresses [20] on the tiny microstructures of the filter caused by ethanol evaporation. After fabrication, a morphological characterization of the device was carried out under a digital microscope (Leica DVM2500) and a Field Emission Scanning Electron Microscopy (Zeiss Supra 40 FE-SEM).

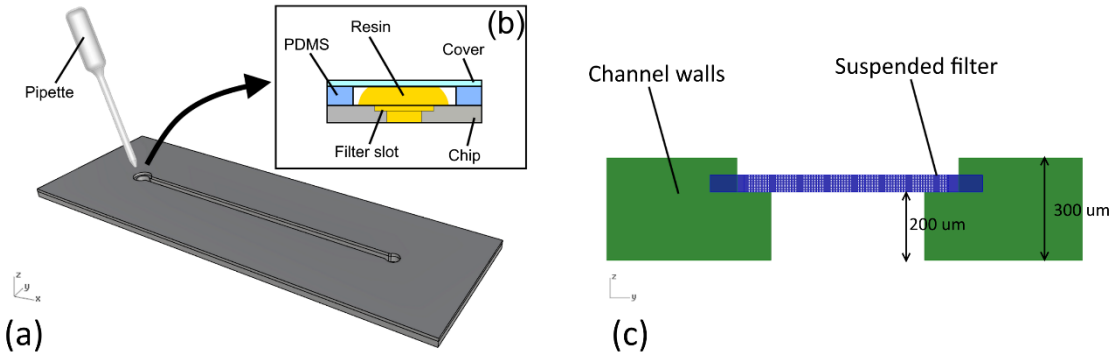

Figure 2 Preparation details before 2PP of the filter: (a) resin is dropped in the chip inlet and (b) resin is flattened by a properly positioned coverslip. No supports are used for filter printing (c).

2.5 Chip enclosure

Since the microfluidic chips had open channels, a specific enclosure was designed in order to close the channel on bottom and on top allowing the controlled flow of a liquid. PDMS was selected as the material for the sealing, since it is non-toxic (it can be used for biologic applications [22–24]) and hydrophobic [25] (helps to contain the liquid flowing in the channel). The mold geometry for the two PDMS sealing layers, top and bottom, was generated in SolidWorks and then realized by Computer Numerically Controlled (CNC) milling into a PMMA slab. After that, PDMS 1:10 was poured in the mold and the two sealing layers obtained after a thermal curing at 90°C for 1 hour.

As showed in Figure 3a, two PMMA plates were added to clamp and keep in position the PDMS sealings with the microfluidic chip inside. Figure 3b shows the final assembly with microfluidic chip inside.

2.6 Fluorescence microscopy tests

The so obtained microfluidic chips were tested to verify their mechanical stability and their efficiency. A fluorescence microscope and FluoSpheres® polystyrene particles (FPs), by Thermofisher, were employed to monitor in real time the filter behavior. In detail, a Zeiss Axio Observer A1 microscope was used in combination with a 470 nm light source. The microfluidic assembly was placed on its stage and connected by the outlet to a 250 µl Hamilton Gastight syringe mounted on a programmable syringe pump (NE1000, New Era Syringe Pump) with a 2 mm diameter tube (SMC polyurethane tubing) as reported in Figure 3c. The liquid flow was strategically controlled from the outlet to avoid excessive stresses on the inlet in which the filter was built. The microfluidic channel was filled with deionized water (DIw) by the syringe with 3 µl/min flow rate before FPs insertion. Two FPs dispersions were prepared by adding 3.3 µl of 1 µm and 4 µm FPs respectively

in 1.5 ml of DIw. The FPs dispersions were pipetted at different times to test filtration efficiency. The channel was filled by withdrawing the volume containing the FPs (6 µl) at 3 µl/min with a syringe pump, hence, a flow from the inlet towards the outlet forced the FPs entering the filter and the channel. Finally, once the whole fluorescent dispersion flowed in the microfluidic system, the syringe was programmed to apply DIw infusion with the same flow rate to observe if all the FPs would have exited from the channel and the filter.

The dimensions of the FPs were chosen in accordance with the expected dimension of the printed filter pores to test its selectivity.

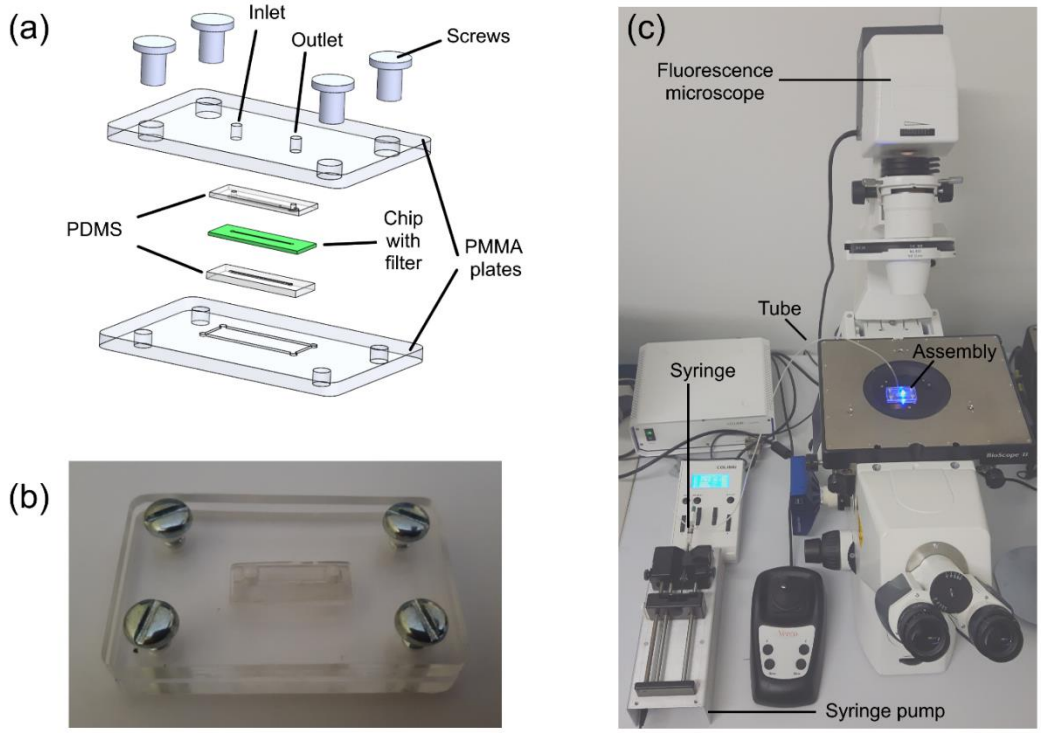

Figure 3 Microfluidic chip tests configuration: (a) exploded view of the clamping assembly; (b) picture of a chip mounted inside the clamping; (c) test setup

3. Results and discussion

In this work the 2PP was combined with a SL printer to fabricate a microfluidic filtration system. Compared to previous works [10,18], the device here reported was entirely built by rapid prototyping techniques and the filter produced in a limited number of process steps. In fact, in the cited studies, the microfluidic chip was developed exploiting clean room technologies [18] or acquired in chip shops [10] and the 2PP was used to obtain the micro filter inside the channels. Other works relying on 2PP features inside an existing device are mainly focused on the study of cells migration [26] and motility [14] rather than sorting.

3.1 Fabrication optimization

The optimized device process combines the SL printing of the microchannel with the micro /nano – 2PP filter fabrication. 2PP step was performed exploiting the high-resolution X,Y plane to reduce the printing time. The novel printing strategy allowed to obtain a final microstructure with a pores size of 4 µm on a considerable area of 0.5 mm^2 in only 30 minutes. The final 3D printed chip is reported in Figure 4a. Observing the microfluidic inlet with a digital microscope it was possible to verify the presence of the step-like feature for the filter integration (Figure 4b). Figure 4c shows the FESEM image of the filter after printing and post-treatment, which is characterized by nanometric features (Figure 4d). The FESEM imaging revealed that the pores in the range 4 – 5 µm were completely opened. With respect to previous works [15,16], the adopted printing strategy allowed the use of an objective without oil immersion and with lower magnification and NA, hence the printing time was shorter while the resolution was preserved. The microfluidic chip and microfilter

structure (s*ee paragraphs 2.1 and 2.2*) were properly designed to simplify and speed up the fabrication process. Indeed, it is known that this kind of printing processes suffer from poor vertical resolution caused by the so-called z-overcure or print through error [27]. Therefore, since the most relevant feature of the filter was the pore dimension, the filtrating surface was oriented along the X,Y plane so as to exploit the better polymerization resolution along such direction and avoid problems of pore clogging caused by print-through phenomenon. A further benefit was the use of a 50x magnification lens with lower numerical aperture, which implies faster printing times than in the case when higher magnifications are employed [28]. Moreover, lower magnification means the possibility to exploit longer working distance and, therefore, enhanced printing flexibility.

The printed chips were stored by fixing them on a glass slide in a proper closed sample holder. Despite the presence of nanometric structures and two different types of materials linked together, the devices could be preserved with no modifications for at least six months at room temperature. This was a first proof of mechanical robustness and good integration between the microfluidics and the filter.

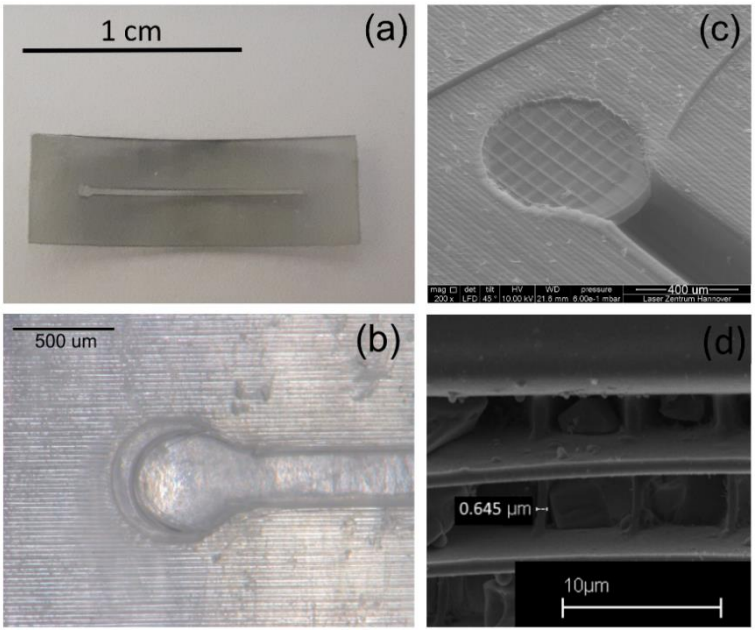

Figure 4 Images of the device at different manufacturing steps: (a) the microfluidic chip after post-curing; (b) detail of the filter slot inside the microfluidic inlet; (c) FESEM image of the filter integrated in the inlet; (d) detail of the nanometric filter features. The visible debris inside the filter pores derives from filter handling during characterization.

3.2 Fluorescence microscopy tests

One of the aims of this study was to evaluate if the two-photon polymerized filter integrated in the SL printed channel could withstand a liquid flow carrying micrometric particles and selectively block only some of them. In the first step, when 1 µm FPs dispersion was loaded in the inlet and withdrawn by the syringe pump, it was possible to clearly distinguish the particles moving in the channel towards the outlet (Figure 5a, white arrow designates flow direction). Over time, the intensity of the signal grew inside the filter, indicating that FPs tended to aggregate in clusters and be trapped inside the filter (highlighted by red circle in Figure 5a). Nevertheless, FPs continued to flow inside the channel. Second step was essential to verify if FPs were permanently blocked in the filter: infusing DIw in the channel, a reversal flow was generated, and particles moved correctly from the outlet to the inlet. As time passed, it was possible to observe a reduction of light intensity in the filter, demonstrating that particles were gradually removed. At the end of this experiment, after 7 minutes, no light signal came from the filter while it was clearly visible in the PMMA inlet (Figure 5b).

The same experiment was performed with 4 µm FPs setting the same flow parameters. During the infusion of particles in the channel (flow from the inlet to the outlet, Figure 5c) they were clearly visible in the filter pores but, differently from the previous case, when flow was reversed from outlet to inlet (to force the particles get out of the filter), almost no light intensity modification was observed in the filter. Assuming that

7 minutes and 3 µl/min were not enough to remove the bigger particles, DIw was furtherly injected from the outlet at 10 µl/min for 30 min. After that time, fluorescence microscope images confirmed that 4 µm FP were trapped inside the filter pores, as showed in Figure 5d.

FESEM images of the filter reported in Figure 5e demonstrated that 1 µm FPs were small enough to pass undisturbed in the filter, while 4 µm FPs remained trapped inside the pores.

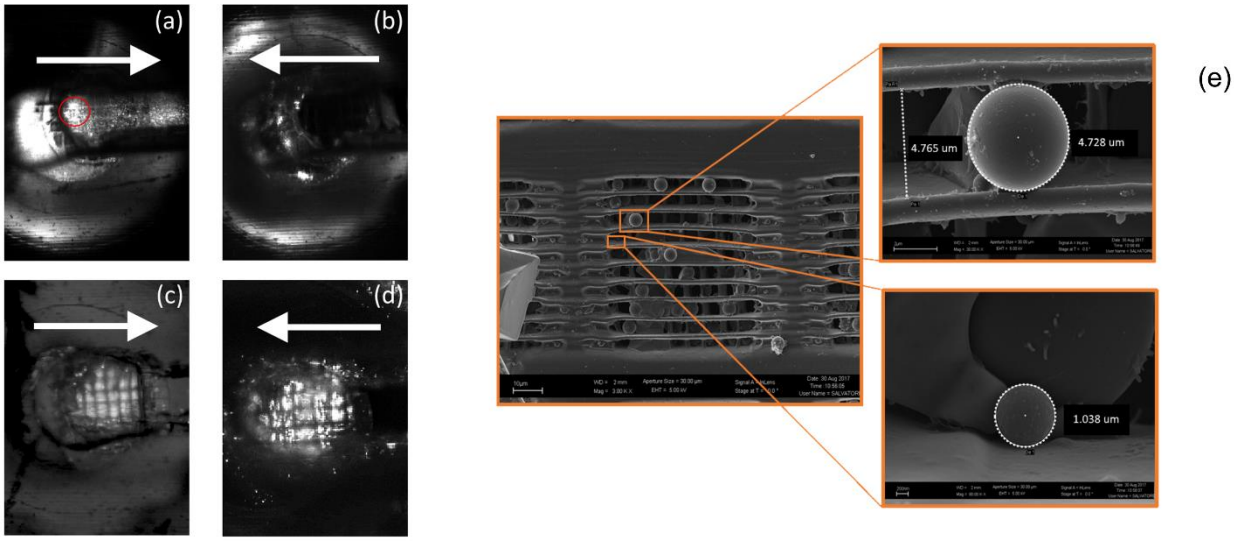

Figure 5 Results from fluorescence tests: (a) the 1 µm FPs flow from the inlet to the outlet; (b) the 1 µm FPs flow from the outlet to the inlet exiting the filter; (c) the 4 µm FPs flow from the inlet to the outlet; (d) the 4 µm FPs flow from the outlet to the inlet with FPs getting trapped inside the filter; (e) FESEM images of the FPs in the filter

4. Conclusions

The microfluidic filtration system developed in this study was designed to be used on a wide range of cells sorting/filtration as, for example, the blood cells. It is composed by two main parts: a micrometric channel, obtained by SL, and a 4 µm pore filter integrated in the channel inlet by 2PP. An accurate and well-studied design allowed to develop a novel additive manufacturing printing strategy to speed up the 2PP fabrication step. Combining information like printing resolution (to orientate the object in the most convenient way) and post-processing drawbacks (to create resistant structures and avoid post-processing failures), it was possible to 3D print a filter with few hundreds nanometer walls able to withstand flows up to 10 µl/min without damages. The filter design involved also the configuration of the micrometric channel, in particular of the inlet, to obtain a satisfying final integration. This was possible thanks to the introduction of a customized microfluidics built by SL rather than a commercial microfluidic chip.

The particle tracking tests confirmed that it is possible to filter 4 µm size FPs, while smaller ones could easily pass without clogging issues. Future works will be focused on the fabrication of more complex filtration systems to be tested with actual biological samples and to finally achieve a multi separation device, able to work from micrometer-size cells to nano vesicles (i.e. exosomes).

More information

Conflicts of interest: none
This research did not receive any specific grant from funding agencies in the public, commercial, or not-for-profit sector.

References

[1] C. Wyatt Shields IV, C.D. Reyes, G.P. López, Microfluidic cell sorting: a review of the advances in the separation of cells from debulking to rare cell isolation, Lab Chip. 15 (2015) 1230–1249. doi:10.1039/C4LC01246A.

[2] A.A.S. Bhagat, H. Bow, H.W. Hou, S.J. Tan, J. Han, C.T. Lim, Microfluidics for cell separation, Med. Biol. Eng. Comput. 48 (2010) 999–1014. doi:10.1007/s11517-010-0611-4.
[3] P. Abgrall, A.-M. Gué, Lab-on-chip technologies: making a microfluidic network and coupling it into a complete microsystem—a review, J. Micromechanics Microengineering. 17 (2007) R15–R49. doi:10.1088/0960-1317/17/5/R01.
[4] D.R. Gossett, W.M. Weaver, A.J. MacH, S.C. Hur, H.T.K. Tse, W. Lee, H. Amini, D. Di Carlo, Label-free cell separation and sorting in microfluidic systems, Anal. Bioanal. Chem. 397 (2010) 3249–3267. doi:10.1007/s00216-010-3721-9.
[5] X. Yang, J.M. Yang, Y.C. Tai, C.M. Ho, Micromachined membrane particle filters, Sensors Actuators, A Phys. 73 (1999) 184–191. doi:10.1016/S0924-4247(98)00269-6.
[6] H.M. Ji, V. Samper, Y. Chen, C.K. Heng, T.M. Lim, L. Yobas, Silicon-based microfilters for whole blood cell separation, Biomed. Microdevices. 10 (2008) 251–257. doi:10.1007/s10544-007-9131-x.
[7] S. Kawata, H.B. Sun, T. Tanaka, K. Takada, Finer features for functional microdevices, Nature. 412 (2001) 697–698. doi:10.1038/35089130.
[8] C. Eschenbaum, D. Großmann, K. Dopf, S. Kettlitz, T. Bocksrocker, S. Valouch, U. Lemmer, Hybrid lithography: Combining UV-exposure and two photon direct laser writing, Opt. Express. 21 (2013) 29921. doi:10.1364/OE.21.029921.
[9] D. Wu, Q.-D. Chen, L.-G. Niu, J.-N. Wang, J. Wang, R. Wang, H. Xia, H.-B. Sun, Femtosecond laser rapid prototyping of nanoshells and suspending components towards microfluidic devices, Lab Chip. 9 (2009) 2391. doi:10.1039/b902159k.
[10] L. Amato, Y. Gu, N. Bellini, S.M. Eaton, G. Cerullo, R. Osellame, Integrated three-dimensional filter separates nanoscale from microscale elements in a microfluidic chip, Lab Chip. 12 (2012) 1135. doi:10.1039/c2lc21116e.
[11] V. Bertana, C. Potrich, G. Scordo, L. Scaltrito, S. Ferrero, A. Lamberti, F. Perrucci, C.F. Pirri, C. Pederzolli, M. Cocuzza, S.L. Marasso, 3D-printed microfluidics on thin poly(methyl methacrylate) substrates for genetic applications, J. Vac. Sci. Technol. B Nanotechnol. Microelectron. 36 (2018). doi:10.1116/1.5003203.
[12] S.L. Marasso, G. Canavese, M. Cocuzza, Cost efficient master fabrication process on copper substrates, Microelectron. Eng. 88 (2011) 2322–2324. doi:10.1016/j.mee.2011.02.023.
[13] S.L. Marasso, D. Mombello, M. Cocuzza, D. Casalena, I. Ferrante, A. Nesca, P. Poiklik, K. Rekker, A. Aaspollu, S. Ferrero, C.F. Pirri, A polymer Lab-on-a-Chip for genetic analysis using the arrayed primer extension on microarray chips, Biomed. Microdevices. 16 (2014) 661–670. doi:10.1007/s10544-014-9869-x.
[14] S. Hengsbach, A.D. Lantada, Rapid prototyping of multi-scale biomedical microdevices by combining additive manufacturing technologies, Biomed. Microdevices. 16 (2014) 617–627. doi:10.1007/s10544-014-9864-2.
[15] J. Wang, Y. He, H. Xia, L.-G. Niu, R. Zhang, Q.-D. Chen, Y.-L. Zhang, Y.-F. Li, S.-J. Zeng, J.-H. Qin, B.-C. Lin, H.-B. Sun, Embellishment of microfluidic devices via femtosecond laser micronanofabrication for chip functionalization, Lab Chip. 10 (2010) 1993. doi:10.1039/c003264f.
[16] D. Wu, S.Z. Wu, J. Xu, L.G. Niu, K. Midorikawa, K. Sugioka, Hybrid femtosecond laser microfabrication to achieve true 3D glass/polymer composite biochips with multiscale features and high performance: The concept of ship-in-a-bottle biochip, Laser Photonics Rev. 8 (2014) 458–467. doi:10.1002/lpor.201400005.
[17] S. Waheed, J.M. Cabot, N.P. Macdonald, T. Lewis, R.M. Guijt, B. Paull, M.C. Breadmore, 3D printed microfluidic devices: enablers and barriers, Lab Chip. 16 (2016) 1993–2013. doi:10.1039/C6LC00284F.
[18] T. Baldacchini, V. Nuñez, C.N. LaFratta, J.S. Grech, V.I. Vullev, R. Zadoyan, Microfabrication of three-dimensional filters for liposome extrusion, in: H. Helvajian, A. Piqué, M. Wegener, B. Gu (Eds.), 2015: p. 93530W. doi:10.1117/12.2083903.
[19] M. Farsari, B.N. Chichkov, Materials processing: Two-photon fabrication, Nat. Photonics. 3 (2009) 450–452. doi:10.1038/nphoton.2009.131.
[20] S. Maruo, T. Hasegawa, N. Yoshimura, Single-anchor support and supercritical CO2 drying enable high-precision microfabrication of three-dimensional structures., Opt. Express. 17 (2009) 20945–20951. doi:10.1364/OE.17.020945.
[21] I.H. Jafri, H. Busta, S.T. Walsh, Critical point drying and cleaning for MEMS technology, in: R.A. Lawton, W.M. Miller, G. Lin, R. Ramesham (Eds.), MEMS Reliab. Crit. Sp. Appl., International

Society for Optics and Photonics, 1999: pp. 51–58. doi:10.1117/12.359371.
[22] D. Huh, G.A. Hamilton, D.E. Ingber, From 3D cell culture to organs-on-chips, Trends Cell Biol. 21 (2011) 745–754. doi:10.1016/j.tcb.2011.09.005.
[23] S.L. Marasso, A. Puliafito, D. Mombello, S. Benetto, L. Primo, F. Bussolino, C.F. Pirri, M. Cocuzza, Optimized design and fabrication of a microfluidic platform to study single cells and multicellular aggregates in 3D, Microfluid. Nanofluidics. 21 (2017) 29. doi:10.1007/s10404-017-1872-0.
[24] C. Potrich, V. Vaghi, L. Lunelli, L. Pasquardini, G.C. Santini, C. Ottone, M. Quaglio, M. Cocuzza, C.F. Pirri, M. Ferracin, M. Negrini, P. Tiberio, V. De Sanctis, R. Bertorelli, C. Pederzolli, OncomiR detection in circulating body fluids: a PDMS microdevice perspective, Lab Chip. 14 (2014) 4067–4075. doi:10.1039/C4LC00630E.
[25] D. Bodas, C. Khan-Malek, Hydrophilization and hydrophobic recovery of PDMS by oxygen plasma and chemical treatment-An SEM investigation, Sensors Actuators, B Chem. 123 (2007) 368–373. doi:10.1016/j.snb.2006.08.037.
[26] M.H. Olsen, G.M. Hjortø, M. Hansen, Ö. Met, I.M. Svane, N.B. Larsen, In-chip fabrication of free-form 3D constructs for directed cell migration analysis, Lab Chip. 13 (2013) 4800. doi:10.1039/c3lc50930c.
[27] T. Baldacchini, Three-dimensional microfabrication using two-photon polymerization : fundamentals, technology, and applications, 2016. https://books.google.com/books?id=D-KoBAAAQBAJ&pg=PA24&lpg=PA24&dq=sla+photobleaching&source=bl&ots=tRB45DHfWV&sig=eMM4-NL-MbWtPV6qH5VhRE0pKu4&hl=en&sa=X&ved=0ahUKEwj52tvE-8vYAhVBTGMKHZviC3EQ6AEIJzAA#v=onepage&q=sla photobleaching&f=false (accessed January 25, 2018).
[28] T. Weiß, G. Hildebrand, R. Schade, K. Liefeith, Two-Photon polymerization for microfabrication of three-dimensional scaffolds for tissue engineering application, Eng. Life Sci. 9 (2009) 384–390. doi:10.1002/elsc.200900002.